Global Analysis of Envisat RA-2 Burst Mode Echo Sequences

Philippa A. M. Berry, Jennifer A. Freeman, Catherine Rogers, and Jérôme Benveniste

***Abstract*—The Envisat RA-2 burst echoes are being gathered throughout the mission; however, these data are only now being made generally available by the European Space Agency. Considerable work has been necessary to turn these engineering-level data into a useable altimeter product. This paper documents the processing steps undertaken to generate usable data and presents the first extensive analysis of this unique dataset, using over 75 000 burst sequences with a global distribution. The results show that the burst echo data from Envisat are of extremely low noise, which is particularly evident over non-ocean surfaces, and contain a wealth of detailed information from both land and ocean surfaces. Examples illustrate the complexity of surface response from targets such as inland water and rough terrain. These unique data clearly have the potential to inform future instrument design as well as to improve the understanding of existing altimeter datasets.**

***Index Terms*—Earth, radar altimetry.**

I. Introduction

OVER THE past two decades, several altimeter-bearing satellites have been launched. These instruments have collected a huge database of echoes from ocean, land, and ice surfaces, which continues to inform the scientific community. One design characteristic of these instruments is the averaging of a substantial number of the individual echoes (IEs) collected along track to form the mean echo which is telemetered to ground, reducing both the required bandwidth and the echo noise (e.g., [1]). Uniquely, the Envisat RA-2, in addition to returning echoes at 18 Hz (equivalent to a nominal along-track spacing of 369 m), has a facility which allows a small proportion of the collected echoes to be telemetered to ground at full 1800-Hz resolution [2] (along-track spacing of 3.69 m). The theoretical extent of a burst is 2000 individual waveforms, the first 16 of which are, in fact, absent for processing reasons, leaving 1984 individual waveforms in a burst sequence. The quantity and geographic distribution of these bursts are constrained by bandwidth; the default programming transmits 1 s of full-resolution echoes every 180 s and obtains bursts from successive cycles from similar locations (unless background activity has been interrupted by a specific user request).

Manuscript received January 30, 2007; revised May 4, 2007.

P. A. M. Berry and J. A. Freeman are with the Earth and Planetary Remote Sensing Laboratory, De Montfort University, LE1 9BH Leicester, U.K.

C. Rogers is with SciSys Ltd., SN14 0GB Wiltshire, U.K.

J. Benveniste is with the European Space Research Institute, European Space Agency, 00044 Frascati, Italy.

Digital Object Identifier 10.1109/TGRS.2007.902280

II. Dataset Preprocessing

A. Initial Processing

In this section, the equations and processing steps required to generate usable IE data from raw data are summarized from the multiple sources in which partial information is available.

The IE data are collected onboard as sets of 128 I, Q pairs per IE represented as

$$X(i) = I(i) + jQ(i)$$

with the bin number $i = 0, \ldots, 127$ and $j = \sqrt{-1}$.

These are first processed through a series of steps which mimic the onboard processing performed on the averaged echoes. The "RAIES" (Radar Altimeter Individual Echoes System) processor performs the following.

1) Multiplication of the I, Q pairs by a Hamming weighting across the 128 samples

$$X_W(i) = W_{\mathrm{H}}(i)X(i)$$

where $W_{\mathrm{H}}(i) = 0.08 + 0.92[\cos(\pi(i-63))/128)]^2$.

2) Application, in the Fourier domain, of the instrument Rx (receive) fine delay (Rx_dis_f) calculated by the onboard Alpha-Beta Tracker

$$X_R(i) = X_W(i) \exp\left[j\frac{2\pi}{128}\frac{i \cdot \text{Rx\_dist\_}f}{64}\right].$$

3) One-dimensional Fourier transform across the 128 I, Q pairs

$$X_{\mathrm{F}}(k) = \frac{1}{128}\sum_{i=0}^{127} X_R(i) \cdot \exp\left[-j\frac{2\pi}{128} \cdot k \cdot i\right].$$

4) Modulus (P) and phase (ψ) extraction from the transformed value X_{F}

$$P(k) = |X_{\mathrm{F}}(k)|^2$$

$$\Psi(k) = \mathrm{atan2}\left[\frac{X_{\mathrm{F}}(k)_{\mathrm{imag}}}{X_{\mathrm{F}}(k)_{\mathrm{real}}}\right].$$

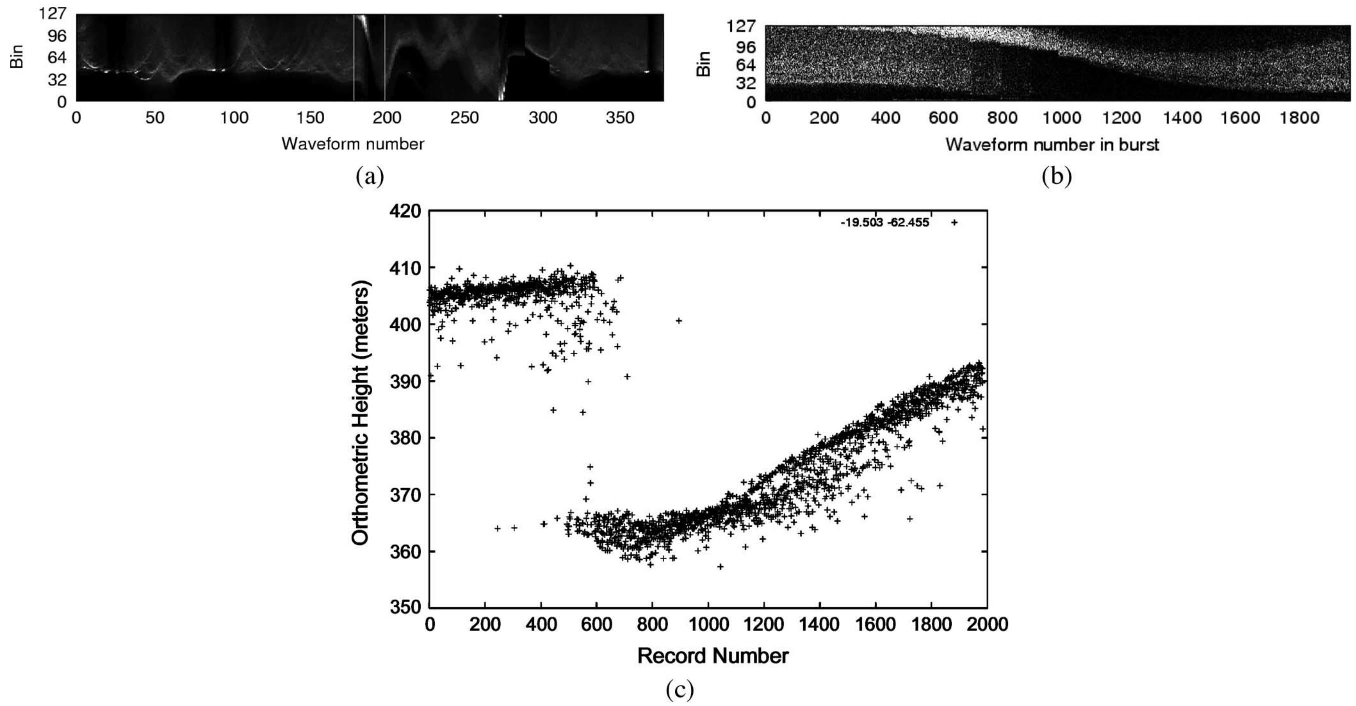

Fig. 1. (a) 18-Hz SGDR waveforms centered at 19.5S, 62.5W [lines show the location of the burst echo sequence given in (b)]. (b) Visualization of burst echo sequence over rough terrain at 19.5S, 62.5W. (c) Height profile of data from (b).

5) Automatic fine gain compensation calculated from onboard parameters and ground calibration tables

$$P_c(k) = \left[\frac{P(k)}{(\text{AGC\_}f)}\right]$$

where AGC_f is the fine gain calculated for the whole waveform.

B. Further Processing

Level 1B waveforms are then produced by the multiplication of the signal by the intermediate frequency (IF) mask, which are uniquely determined for each echo for correction of power distortions, whereas the 18-Hz product calculates and applies a single IF mask to the averaged waveform. The significance of this is seen when IE waveforms are averaged to reconstruct a corresponding 18-Hz waveform; the results will not be identical. The processor also calculates other parameters at 1800 Hz, including the total window delay. The window delay is the two-way travel time of the radar pulse from the satellite to the surface and back; this measurement is referenced to the center of the range window. The window is the fast Fourier transform gates onboard the instrument, which effectively gives a window of range to surface within which to "catch" the returned echo.

The range-to-surface and instrument AGC parameters are updated at 18 Hz (100 individual waveforms) onboard the RA-2. This introduces apparent "sawtooth" artifacts and power steps in IE waveform sequences [Fig. 1(b)]. This is particularly apparent when the underlying topography is changing rapidly. To compensate for these artifacts, the RAIES processor generates a "window delay" for each of the IE from which a range can be computed.

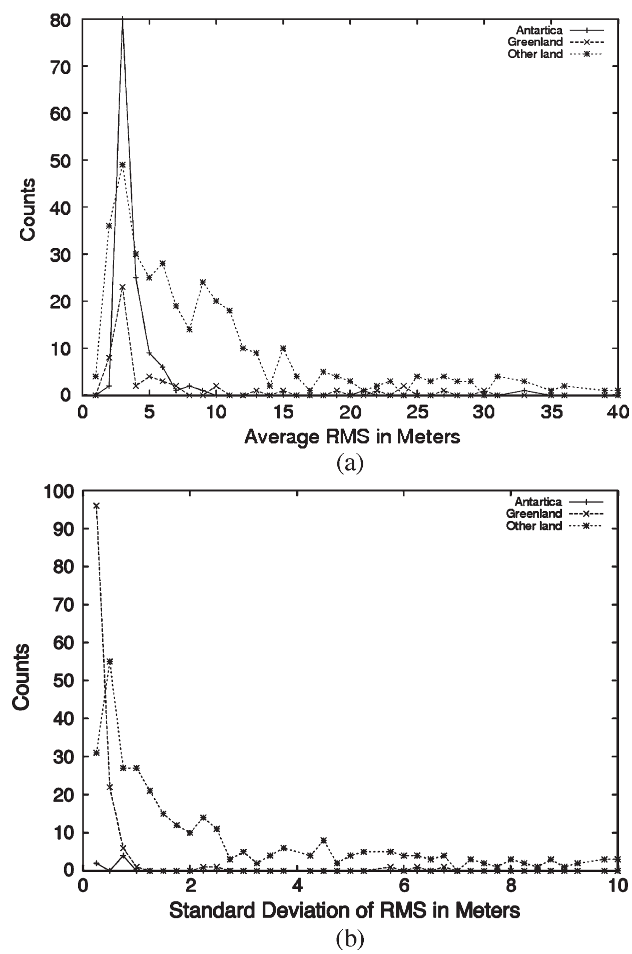

Fig. 2. (a) Distributions of collocated burst echo mean rms over land surfaces in meters. (b) Distributions of collocated burst echo standard deviation of rms over land surfaces in meters.

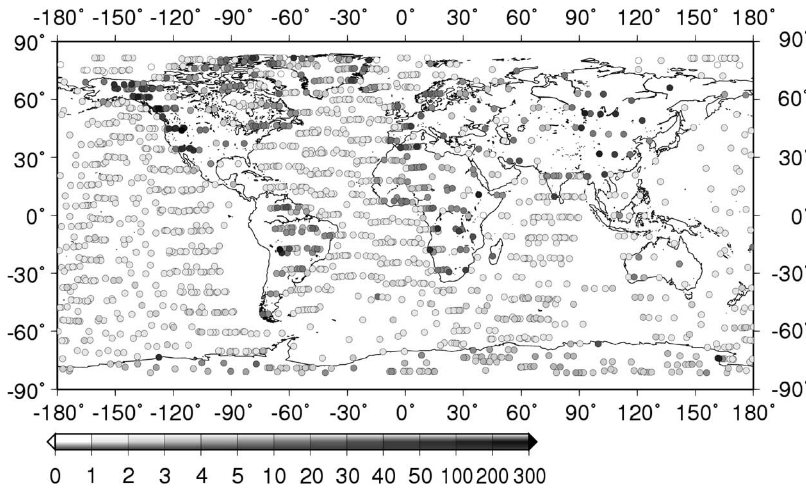

Fig. 3. Global location and mean rms of collocated burst echoes over all surfaces in meters.

Sawtooth artifacts are illustrated in Fig. 1(b), where a burst sequence obtained over rapidly varying terrain [its location within the 18-Hz sequence is shown in Fig. 1(a)], has been retracked using the expert system [3] with the range calculated for each echo [Fig. 1(c)].

As is generally the case when using radar altimeter data, a series of corrections to the range must be applied for each measurement, including atmospheric propagation (wet + dry troposphere, ionosphere) [4]. Note that, at present, orbit data must be retrieved from a source other than the Level 1B data, as there is currently an unacceptably high level of error in the satellite altitude at Level 1B. In this paper, therefore, we have collocated the data with the corresponding sensor geophysical data records (SGDR) [2] from which all range corrections and orbit data have been obtained.

In this paper, echoes were reprocessed globally for ten cycles (cycles 33 to 42) to investigate the annual variability; this huge dataset containing 75 120 bursts was then analyzed to determine the information content.

III. Analysis

As indicated by the first results using sample data from one 35-day cycle [5], [6], the noise was found to be consistently very low, permitting meaningful analysis and retracking to be performed at full 1800-Hz resolution over non-ocean surfaces. Over the open ocean, the noise on these echoes [5] is too great to permit a full Brown [7] model fit to be performed for a single IE. Note that averaging has not been performed for the information content analysis in this paper.

A. Non-Ocean Surfaces

Non-ocean surfaces are often highly variable, even within the spatial scale of successive 18-Hz waveforms (about 369 m). The low reflectivity to radar of much of the land surface at Ku-band [8] means that most of the power received by the altimeter is returned from surfaces close to the nadir point. To investigate the high-frequency information content of the burst echoes, the rms of the retracked heights about the mean was calculated for each set of 100 echoes, corresponding to the 18-Hz SGDR dataset. Statistics were then generated for each burst. Because the bursts occur in approximately the same

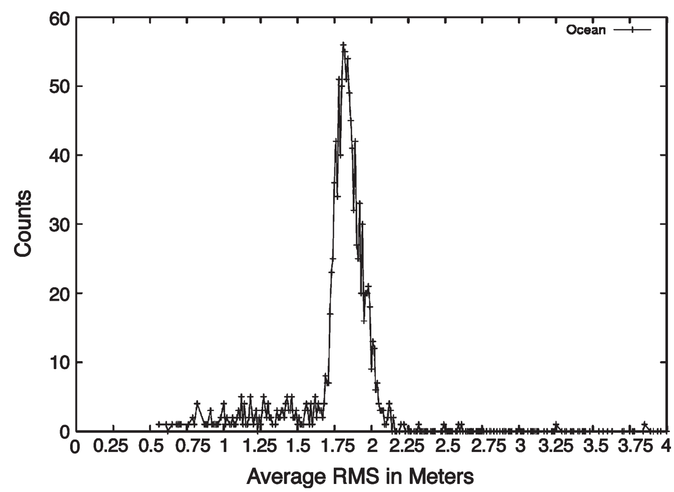

(a)

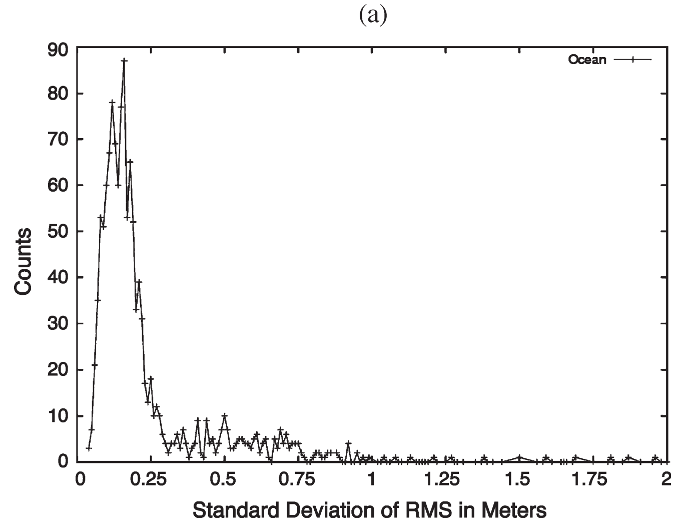

(b)

Fig. 4. (a) Distribution of collocated burst echo mean rms over ocean in meters. (b) Distribution of collocated burst echo standard deviation of rms over ocean in meters.

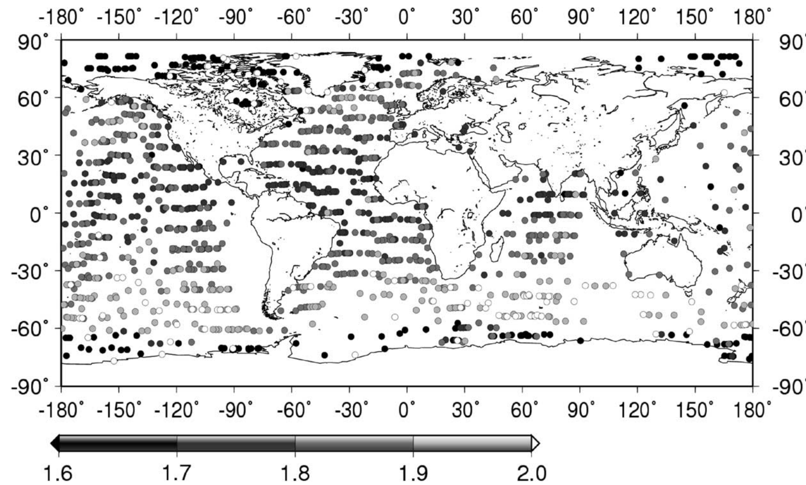

Fig. 5. Global location and mean rms of collocated burst echoes over ocean in meters.

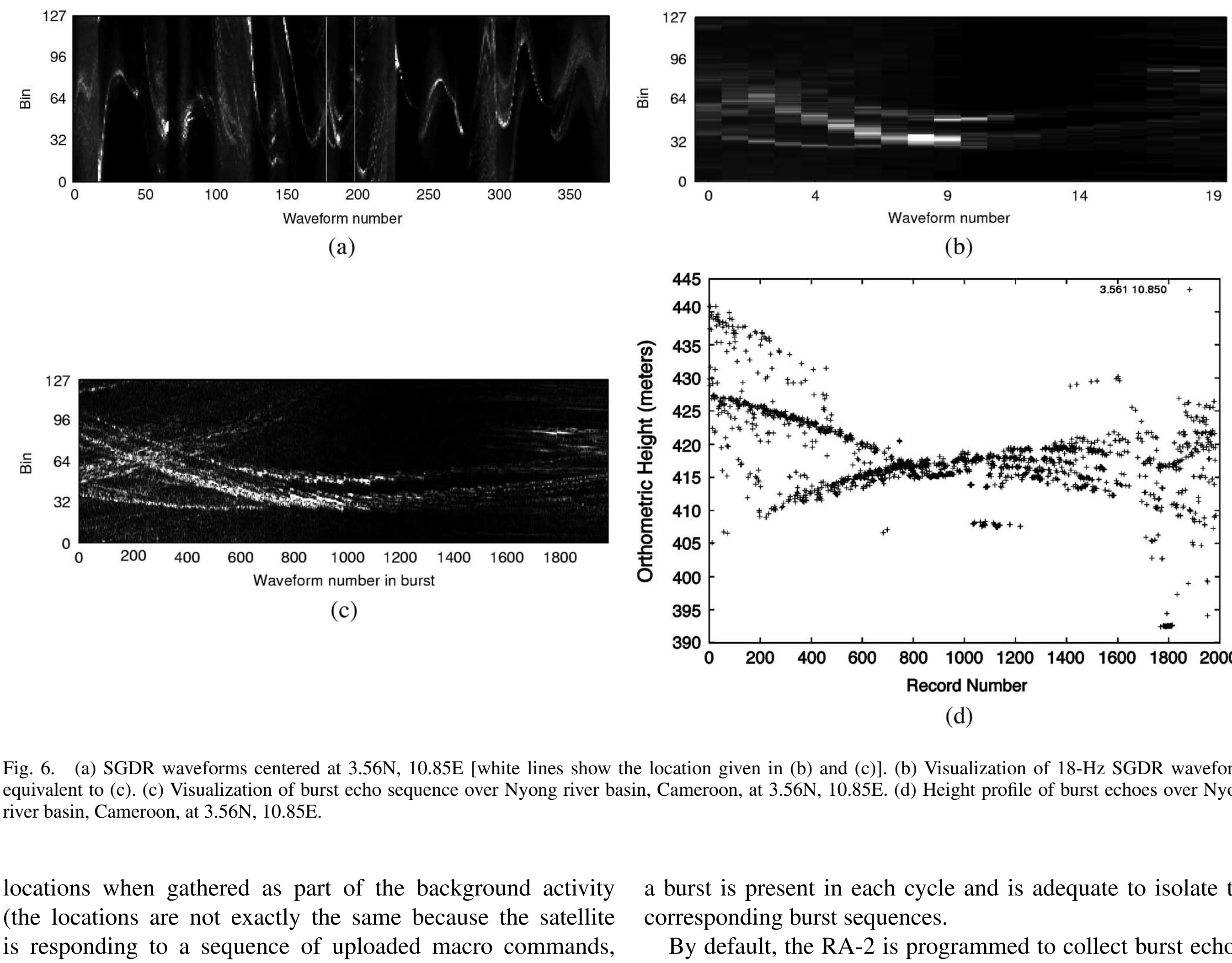

Fig. 6. (a) SGDR waveforms centered at 3.56N, 10.85E [white lines show the location given in (b) and (c)]. (b) Visualization of 18-Hz SGDR waveforms equivalent to (c). (c) Visualization of burst echo sequence over Nyong river basin, Cameroon, at 3.56N, 10.85E. (d) Height profile of burst echoes over Nyong river basin, Cameroon, at 3.56N, 10.85E.

locations when gathered as part of the background activity (the locations are not exactly the same because the satellite is responding to a sequence of uploaded macro commands, and small variations in timing execution occur), data from successive cycles were collocated using the average location for each burst, and time series of these statistics was generated globally. The criteria used were the following. The echoes were within 0.1° radius of each other, and the echoes had the correct relative pass number. While the degree size does change with latitude, this approximation is sufficient to determine if a burst is present in each cycle and is adequate to isolate the corresponding burst sequences.

By default, the RA-2 is programmed to collect burst echoes in approximately the same location cycle to cycle; however, users may request the European Space Agency (ESA) to acquire a burst sequence at a specific location along the orbit. When this occurs, the positions of subsequence bursts are affected. In this paper, data were specifically selected from a period when no such user requests had disturbed the normal background activity of the RA-2.

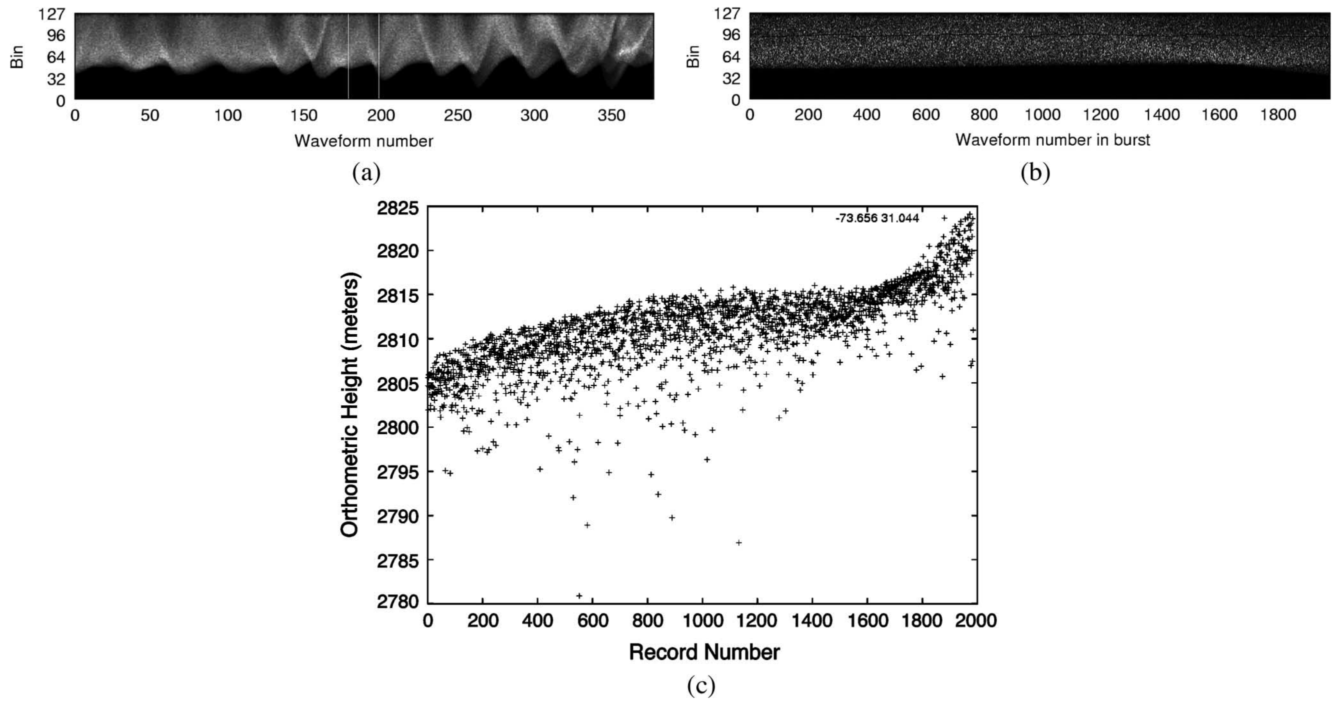

Fig. 7. (a) SGDR waveforms centered at 73.656S, 31.044E [white lines show the location given in (b)]. (b) Visualization of burst echo sequence over Antarctica at 73.66S, 31.04E. (c) Height profile of burst echoes over Antarctica at 73.66S, 31.04E.

The mean and standard deviation of the burst rms for this year of data were calculated for each derived land location and histograms [Fig. 2(a)]. Land ice shows a narrower distribution than other land responses consistent with the generally slowly varying terrain over both Antarctica and Greenland; the observed differences in the distributions for Antarctica and Greenland are a consequence of the nonuniform locations of the bursts and the shape of these land masses. The geographic distribution of the mean rms data was then plotted (Fig. 3); the rms is naturally highest over mountains. Less obvious is the significant rms of bursts over inland water, which is discussed in Section III-C. The temporal variation in rms [Fig. 2(b)] is naturally highest over mountainous terrain, where small changes in the burst location cause the terrain to be sampled differently.

B. Oceans

The distribution of mean rms and its standard deviation for the year over oceans was derived [Fig. 4(a)]. Here, the main distribution of rms shows the response of the open ocean. Note that these rms results are primarily derived from heights based on threshold retracking in contrast to the more precise retracking available in the SGDR dataset, where waveforms are processed with a Brown model fit which significantly enhances the vertical precision of measurement.

Analyzing the geographical distribution of these data over the oceans (Fig. 5) shows the low variation around the equator and the very high values in the south circumpolar current. The low rms in the presence of sea ice is evident, the effect greatest in the northern hemisphere in the presence of multiyear ice. The standard deviation also shows irregularities in distribution

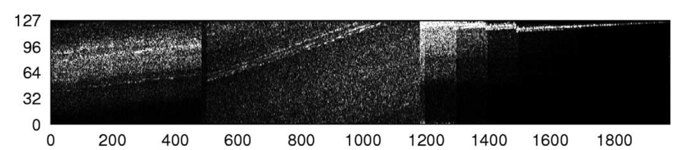

Fig. 8. Visualization of burst echo sequence with nonoptimal mode change at 2.43N, 30.15E.

[Fig. 4(b)], with the single year ice in the southern hemisphere contributing to a higher variation in rms.

C. Sample Burst Results

From these global results, sample data were selected to illustrate the detailed information available from the burst echoes.

As expected over mountainous terrain, the range is rapidly changing even within a single burst echo sequence; this is illustrated by an example over the Andes (Fig. 1) which shows that the retracked height is following the distribution of power within the waveform and moves from the higher surface to the lower when the lower surface dominates the returned power.

The burst echo rms shows high variability globally over inland water. The primary contributing factor is illustrated by an example from the Nyong river basin in Cameroon (Fig. 6). Here, the presence of a large number of quasi-specular targets within the pulse-limited footprint causes multiple off-ranging arcs to appear in the retracked orthometric heights [Fig. 6(d)]. This shows that the complex response of inland water apparent at 10–20 Hz [9] is equally evident at the smaller spatial scale available with 1800-Hz data, with multiple reflecting facets contributing to the altimeter returns [Fig. 6(c)]; many of these signals are blurred at the sampling rates of 18 Hz [Fig. 6(b)] available in the SGDR product, or they appear in only one or two successive echoes [Fig. 6(a)] and are not easily identified as inland water components.

Over gradually varying high reflectance topography such as land ice, some averaging of the burst echoes or the retracked heights may be useful, as illustrated by the scatter present on retracked heights over Antarctica (Fig. 7).

In addition to the scientific data available, the burst echoes can be used to examine engineering-related behavior by providing a very detailed look at the instrument performance on small scales. To illustrate this, Fig. 8 shows a burst sequence during which the RA-2 changes mode (from 80 to 320 MHz, then returning to 80-MHz mode). Visual examination clearly shows that the instrument mode-switching algorithm is not performing optimally in this instance; the instrument switched to a higher resolution mode, immediately lost the leading edge of the waveform, and switched back to the original mode.

IV. Discussion

This first global analysis of over 75 000 burst echo sequences has revealed the presence of a wealth of high-frequency information not available in the 18-Hz dataset. The noise is extremely low, and the quality of the burst echoes is therefore very high as is evident in comparisons between the 18- and 1800-Hz data. Some averaging of data from slowly varying surfaces, such as ocean, may be appropriate. However, many land targets show relatively poor reflectance at this frequency, which results in the returned echo being dominated by a small patch on the surface situated directly below the instrument at nadir. In consequence, high-frequency information is present in many burst echo sequences over land. These data provide a forensic tool for the detailed investigation of the response of complex targets such as inland water. With these data shortly being made available by ESA to the user community in an SGDR-type format with full corrections included [10], they can now be utilized to provide a valuable forecast of the information from future missions and to influence instrument design.

References

[1] A. R. Zieger, D. W. Hancock, G. S. Hayne, and C. L. Purdy, "NASA radar altimeter for the TOPEX/POSEIDON Project," *Proc. IEEE*, vol. 79, no. 6, pp. 810–826, Jun. 1991.

[2] J. Benveniste *et al.*, *ENVISAT RA-2/MWR Product Handbook*. Frascati, Italy: Eur. Space Agency, 2002. Issue 1.2, PO-TN-ESR-RA-0050.

[3] P. A. M. Berry, A. Jasper, and H. Bracke, "Retracking ERS-1 altimeter waveforms over land for topographic height determination: An expert system approach," *ESA Pub*, vol. SP-414, no. 1, pp. 403–408, 1997.

[4] R. Scharroo, "A decade of ERS satellite orbits and altimetry," Ph.D. dissertation, Delft Univ. Technol., Delft Univ. Press, Delft, The Netherlands, 2002.

[5] P. A. M. Berry, C. Rogers, J. D. Garlick, J. A. Freeman, and J. Benveniste, "The envisat burst mode echoes—A new look from satellite radar altimetry," in *Proc. "15 Years Progress Radar Altimetry" Symp.*, 2006.

[6] C. Gommenginger, P. Challenor, J. Gomez-Enri, G. Quartley, M. Strokosz, P. Berry, J. Garlick, D. Cotton, D. Carter, C. Roger, S. Haynes, I. LeDuc, M. Milagro, and J. Benveniste, "New scientific applications for ocean, coastal, land and ice remote sensing with Envisat radar altimeter individual echoes," in *Proc. "15 Years Progress Radar Altimetry" Symp.*, 2006.

[7] G. S. Brown, "The average impulse response of a rough surface and its applications," *IEEE Trans. Antennas Propag.*, vol. AP-25, no. 1, pp. 67–74, Jan. 1977.

[8] P. A. M. Berry, J. D. Garlick, and R. G. Smith, "Near-global validation of the SRTM DEM using satellite radar altimetry," *Remote Sens. Environ.*, vol. 106, no. 1, pp. 17–27, Jan. 2007.

[9] P. A. M. Berry, J. D. Garlick, J. A. Freeman, and E. L. Mathers, "Global inland water monitoring from multi-mission altimetry," *Geophys. Res. Lett.*, vol. 32, no. 16, L16401, Aug. 2005. DOI:10.1029/2005GL022814.

[10] ESA, *Envisat Radar Altimeter Individual Echoes*, Apr. 2007. [Online]. Available: http://earth.esa.int/raies

Philippa A. M. Berry received the Ph.D. degree from Aston University, Birmingham, U.K., in 1984.

Following her Postdoctoral positions with Leicester University and University College London, she spent several years in industry working for the Vega Group before moving to De Montfort University, Leicester, U.K., in 1993. During the past eight years, she founded and developed the EAPRS Laboratory, researching primarily in multifrequency satellite radar altimetry, both engineering aspects and analysis, and interpretation of data over all surfaces, including land and inland water.

Prof. Berry is a Fellow of the International Association of Geodesy and Director of the IAG IDEMS Centre. She was awarded a personal Chair by De Montfort University in 1999.

Jennifer A. Freeman is currently working toward the Ph.D. degree on the interpretation of radar altimeter data over the oceans and coastal regions at De Montfort University, Leicester, U.K.

She joined the Earth and Planetary Remote Sensing Laboratory, De Montfort University, as a Programmer.

Ms. Freeman was awarded a First in Software Engineering from De Montfort University in 2004.

Catherine Rogers received the D.Phil. degree in the field of the Earth's magnetosphere simulations from Sussex University, Brighton, U.K., in 1990.

After working at the European Organisation for the Exploitation of Meteorological Satellites for six years, through the commissioning stage of MSG-1, and specializing in image processing, she returned to the U.K., where she is currently working at SciSys Ltd., Wiltshire, U.K., on ground segment design and implementation.

Jérôme Benveniste received the Ph.D. degree from the University of Toulouse, Toulouse, France, in 1989.

After a postdoctoral position at the Massachusetts Institute of Technology, Cambridge, he has been with the European Space Research Institute (also known as the Centre for Earth Observation), European Space Agency (ESA), Frascati, Italy, since 1992, where he is in charge of the ERS-1, ERS-2, and Envisat radar altimeter data exploitation and the Research and Development Projects, including CryoSat, GOCE, and SMOS data exploitation, interacting with ESA Earth Observation Principal Investigators and establishing science requirements for the Sentinel-3 Radar Altimeter.